Journal of Atmospheric and Terrestrial Physics, Vol. 49, Nos. 7/8, pp. 675–687, 1987.
Printed in Great Britain.

0021–9169/87 $3.00 + .00
Pergamon Journals Ltd.

Mean winds in the winter middle atmosphere above northern Scandinavia

W. MEYER
Physikalisches Institut der Universität Bonn, D-5300 Bonn 1, F.R.G.

C. R. PHILBRICK
A.F. Geophysics Laboratory, Hanscom AFB, Bedford, MA 01731, U.S.A.

J. RÖTTGER*
EISCAT Scientific Association, S-981 27 Kiruna, Sweden

R. RÜSTER, H.-U. WIDDEL
Max-Planck-Institut für Aeronomie, D-3411 Katlenburg-Lindau 3, F.R.G.

and

F. J. SCHMIDLIN
NASA Goddard Space Flight Center, Wallops Island, VA 3337, U.S.A.

(*Received for publication* 14 *January* 1987)

Abstract—Wind measurements which were carried out during the MAP/WINE Campaign in northern Scandinavia between 2 December 1983 and 24 February 1984 are used to derive background winds and monthly as well as winter mean values from the ground up to 90 km altitude. These mean winds compare favourably to the wind field proposed for the revised CIRA 86, which is deduced from satellite measurements. The vertical structure of the zonal monthly means is similar in both data sets during January and February. The winter mean zonal winds are observed to be slightly stronger in the stratosphere and lower mesosphere during the MAP/WINE winter than the satellite winds proposed for CIRA 86. The long term mean meridional winds are in good agreement up to 60 km. They indicate a dominant influence of quasi-stationary planetary waves up to 90 km and an ageostrophic poleward flow between 60 km and 85 km over northern Scandinavia, which maximizes at 76 km at about 8 m s^{-1}. The observed short term variability of the wind is discussed with respect to a possible impact of saturating gravity waves on the momentum budget of the middle atmosphere.

1. INTRODUCTION

In winter the middle atmosphere at high latitudes is a region of enhanced dynamic activity. The simultaneous presence of different scales of motion (turbulence, gravity waves, planetary waves, etc.), however, makes it difficult to study the individual types of motion and their importance for the momentum and energy budget, as well as to derive a mean state of the winds. In recent years newly developed radar techniques have improved knowledge of the mesospheric wind structure considerably (RÜSTER, 1984). Unfortunately, these techniques are still limited to a few sites and to certain altitude ranges. Information on the stratospheric wind field is mostly provided by meteorological rocket measurements, however, the bulk of routine measurements has been accumulated on the American continent. Up to now the number of wind measurements from stations in the eastern hemisphere is too scarce near 70° northern latitude to give reliable mean wind information. Hence, there is still a need for more comprehensive coverage of wind information at high latitudes. As part of the MAP/WINE project (VON ZAHN, 1987) considerable efforts were undertaken to observe the middle atmospheric wind field from the Andøya Rocket Range (69.3°N, 16°E), northern Norway, and nearby sites. Different wind measuring techniques, such as meteorological rockets, sounding rockets and two radar systems, provided wind information

*On leave from Max-Planck-Institut für Aeronomie, Katlenburg-Lindau, F.R.G.

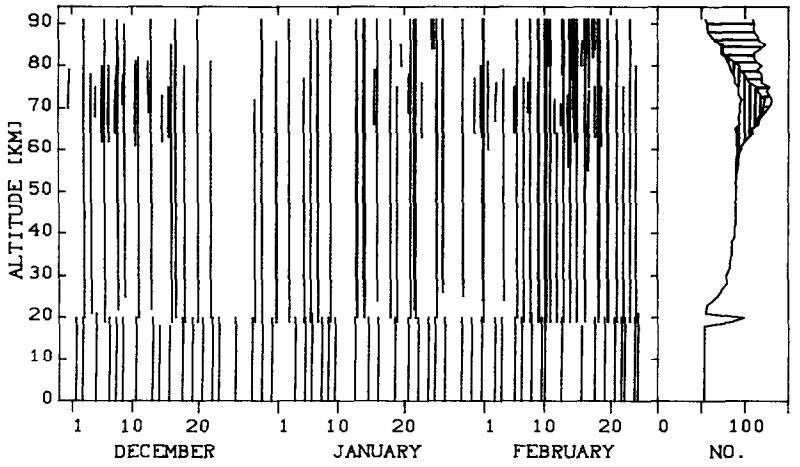

Fig. 1. Distribution in time of wind profiles obtained during the period of rocket launches at Andøya (69°N, 16°E). Total number of measurements used for mean wind reduction (right panel): rocket measurements (blank), MST radar (vertically dashed), EISCAT (horizontally dashed).

throughout the entire altitude range of the middle atmosphere. The main purpose of this paper is to derive the mean state of winds above northern Scandinavia during the period of rocket launches between 2 Dec. 1983 and 24 Feb. 1984 from the ground up to 90 km. We shall subsequently discuss a comparison of our measurements with satellite derived winds as proposed for the revised CIRA 1986 by BARNETT and CORNEY (1985). A comparison between indirectly deduced winds from satellite measurements and wind measurements may be important, because in future emphasis will have to be placed on satellite measurements, which will provide a more global coverage than was possible with meteorological rocket stations.

2. DATA

An overview of all the wind profiles obtained during the principal time period of activities in northern Scandinavia is presented in Fig. 1. Most of the results were obtained using *in situ measuring techniques*, i.e. 57 passive falling spheres, 33 datasondes, 18 foil clouds and 2 instrumented spheres. All payloads were tracked by a precision C-band radar (MPS-36), which is an essential requirement for deriving high quality wind information from the tracks of dropsondes (SCHMIDLIN and MICHEL, 1985). For each launch the track underwent a careful inspection and obviously bad portions were removed before computing the final wind profiles. The foil clouds—also denoted 'chaff'—(WIDDEL, 1987) provided the best vertical resolution of all available wind measurements. In addition to small scale wind examinations in the range 70–86 km these measurements were also used to validate the wind reduction from passive falling spheres at high altitudes. A comparison of wind profiles from chaff and falling spheres showed good agreement—better than expected—and encouraged us to increase the vertical resolution of the wind reduction of passive falling sphere tracks in the mesosphere and upper stratosphere compared to earlier results obtained by SCHMIDLIN *et al.* (1985). The improvement of the vertical resolution goes along with an increase in the error in the derived winds, which has been discussed by MEYER (1985) and SCHMIDLIN and MICHEL (1985). A revised error analysis showed that the error of the horizontal winds derived from passive spheres as given by MEYER (1985) must be corrected to the following estimates: $0.5\,m\,s^{-1}$ (30 km), $1.5\,m\,s^{-1}$ (50 km), $4\,m\,s^{-1}$ (70 km) and $15\,m\,s^{-1}$ (90 km). Datasondes, which carry a thermistor for *in situ* temperature measurements, are equipped with a parachute-like retardation device. Their estimated wind error is similar to the values given above, but they provide a better vertical resolution than passive spheres do. Falling spheres and datasondes were often tracked down to 20 km. Below this altitude the radiosondes of Bodø station (200 km south of Andøya) complemented the wind field down to the sea surface.

Above 60 km *remote measurements* by MST (mesosphere–stratosphere–troposphere) and incoherent scatter radars provided additional important wind information. The mobile MST radar 'SOUSY' (RÜSTER and KLOSTERMEYER, 1987) was located 5 km south of the rocket launch pad, whereas the horizontal distance to the descent trajectory of the rocket payloads

was about 50 km. Echoes were mainly received around noon from the altitude range 60–80 km (CZECHOWSKY *et al.*, 1984). In order to incorporate these measurements into a mean wind reduction, daily height profiles of the wind have been derived from the signal spectra incoherently added over the total operation period for each day. The data are also shown in Fig. 1. A description of the wind measurements by the UHF radar of EISCAT during the winter of MAP/WINE is given by RÖTTGER and MEYER (1987). Zonal wind components were obtained about 20 km south of the rocket payload descent trajectories in the mesosphere. Meridional winds were measured at 200 km distance from the Andøya Rocket Range. For this analysis we are using hourly averages of EISCAT wind measurements. EISCAT was operating in January and February and generally provided accurate wind information above 85 km.

3. PREVAILING WINDS AND MONTHLY MEANS

One objective of the rocket launch schedule was to cover a broad range of temporal scales for the dynamic processes. For this reason launches were performed in short succession (salvoes), which can be recognized in Fig. 1 as thick vertical lines, as well as single measurements that were carried out at regularly spaced intervals between salvoes in order to provide the information for long term changes. These data form the basis for monthly means discussed in this paper. It can be seen from Fig. 1 that the background wind field can be derived continuously on a time scale of about 5 days, except for a 7 day data gap in late December. The wind profiles were averaged over 5 km altitude to suppress some of the short period gravity wave oscillations. Above 70 km the regular semi-diurnal tide has also been removed, following the results obtained by RÖTTGER and MEYER (1987).

The unevenly spaced data points were interpolated to an equally spaced grid at each kilometer altitude. We used a weighted mean of all measurements within a time window of ± 2 days (but at least 3 measurements around a time point) to estimate the trends between the wind measurements. The weights were derived from a smooth estimate of the time structure function—disregarding periodicities—at the time difference between the measurements and the time point to be estimated. The sample time structure function s is defined by

$$s(\tau) = \overline{[u(t)-u(t+\tau)]^2}, \qquad (1)$$

$u(t)$ representing the wind measurement at t and τ being the time lag. The bar denotes an average over all t. The 4 day average of the continuous time series so obtained is assumed to represent mean winds on a time scale of about 5–6 days. Thus, a temporal smoothing was performed in order to suppress short period oscillations, dependent on their expected magnitude at specific altitudes. This procedure is not as sensitive, especially above 85 km, to single measurements at the boundary of data gaps as linear interpolation, which was earlier applied by MEYER *et al.* (1985).

Figure 2 shows the background wind field as a function of time between 0 km and 90 km. The flow had a clear prevailing westerly (from the west) component up to 75 km. Two pronounced maxima of the westerly jet occurred during the winter in the stratopause region: one in the middle of December and one at the end of January and beginning of February. During these times the actual maximum wind speeds frequently exceeded 100 m s^{-1}. During the December storm period wind speeds of 200 m s^{-1} were observed above southern Norway (Lista, 58°N, 7°E) at 55 km altitude. A breakdown of the zonal jet happened in the first half of January in the stratopause level, which, however, seemed not to affect the polar night jet in the lower stratosphere. Winds in the lower stratosphere were observed to decrease and even to reverse to weak easterlies only before and during the major stratospheric warming event on 23 Feb. (LABITZKE *et al.*, 1984) over Andøya. Between 20 Feb. and 24 Feb. strong day-to-day variations of the stratospheric and mesospheric winds were observed over Andøya (Fig. 3). In particular, strong northerly winds of 75 m s^{-1} occurred on 23 February at 1700 UT. Such magnitudes were rarely observed during the winter below 75 km. Note also the continuous change of the vertical slope of the wind direction, which reflects the strong baroclinic vertical structure within the center of the warming. The background flow (Fig. 2) in the upper mesosphere was rather weak between 10 Feb. and the end of our observation period. MULLER *et al.* (1985) and LABITZKE *et al.* (1987) have shown that there exists a strong correlation between the weakening or reversal of the zonal wind over Sheffield (53°N, 2°W) at 95 km and warming events in the high latitude stratosphere during the MAP/WINE winter. At the times of minor warmings around 1 Jan., 22 Jan. and 10 Feb. (LABITZKE *et al.*, 1984) the wind in the upper mesosphere was also observed to weaken over Andøya at 90 km, although this was not strikingly evident.

The meridional wind component exhibited a rather unsystematic behaviour during these times: southerlies around 22 Jan. and northerlies on 1 Jan. and 10 Feb. During December the error bar of 15 m s^{-1} of the background wind is relatively high and values

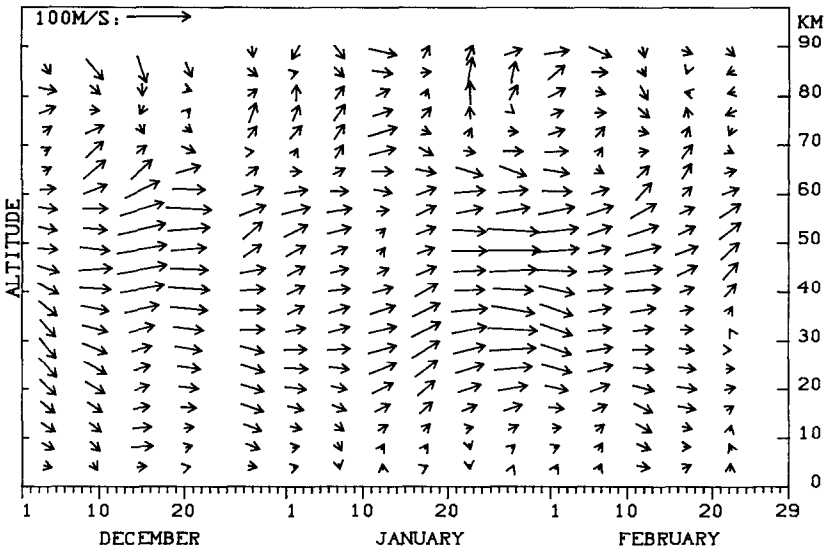

Fig. 2. The estimated prevailing wind field above Andøya. Arrows indicate magnitude and direction of the horizontal flow (from the south: upward, from the west: to the right).

are not shown for 89 km. The error is generally decreasing to values less than 10 m s^{-1} below 80 km and to values less than 5 m s^{-1} below 50 km, although it is only 5 m s^{-1} up to the top level during the middle of February.

Monthly mean winds were derived by averaging the background wind field over the following periods: 3 Dec.–23 Dec. and 28 Dec.–1 Jan. (termed 'December') and 1 Jan.–1 Feb. ('January') and 1 Feb.–23 Feb. ('February'). The results are shown in Fig. 4a for the zonal component. All three profiles agree remarkably well in the upper mesosphere, showing a minimum of 10 m s^{-1} just below 80 km. Below 65 km wave-like fluctuations cause come deviations between the means. The upper west wind maximum was located at 56 km, 51 km and 48 km in December, January and February, respectively. These levels are almost identical with those of the stratospheric mean monthly temperature maxima (OFFERMANN *et al.*, 1987). A second maximum occurs somewhat lower at 44, 31 and 24 km in the same monthly order. Because of the absolute maximum of 48 m s^{-1} at 31 km the shape of the January profile appears to have a more irregular behaviour compared to the December and February winds, which can also be seen in Fig. 2. This irregularity becomes more evident in the meridional monthly mean shown in Fig. 4b. The December and February profiles follow a similar vertical structure up to the mesopause, changing from negative values at 27 km to about +10 m s^{-1} around 60 km and decreasing to negative values again at 80 km. The January profile shows an oppositie vertical structure up to 80 km except for the altitude range 40–60 km, where constant southerly winds of 7 m s^{-1} are observed. In particular note the anticorrelation around 65 km and 85 km among the December and January profiles. From Fig. 2 this anticorrelation is most evident during a time period in the middle of December and the second half of January at these altitude levels. Above 80 km the trend of all three monthly means was towards negative values of −8 m s^{-1} at 90 km.

4. COMPARISON WITH OTHER MEASUREMENTS

The data near 70°N before MAP/WINE is rather scarce for the eastern hemisphere. Only a few *in situ* measurements were available before 1970 (CIRA, 1972). A few more measurements were performed during the Energy Budget Campaign in November 1980 (OFFERMANN, 1985), which, however, do not overlap with our seasonal coverage. Meteor radar measurements of the zonal wind component were performed above 80 km during the first half of February in 1975 over Kiruna (68°N, 21°E) by MASSEBEUF *et al.* (1979). Their result of 10 m s^{-1} at 80 km is in agreement with our February mean, however, they observed a further decrease above 80 km to less than 5 m s^{-1} at 90 km. Similar results were also obtained over Poker Flat (65°N, 147°W) with an MST radar in this altitude range (MANSON *et al.*, 1985). Measurements from Poker Flat in the mesosphere were given by BALSLEY *et al.* (1983) for January 1980. These authors observed

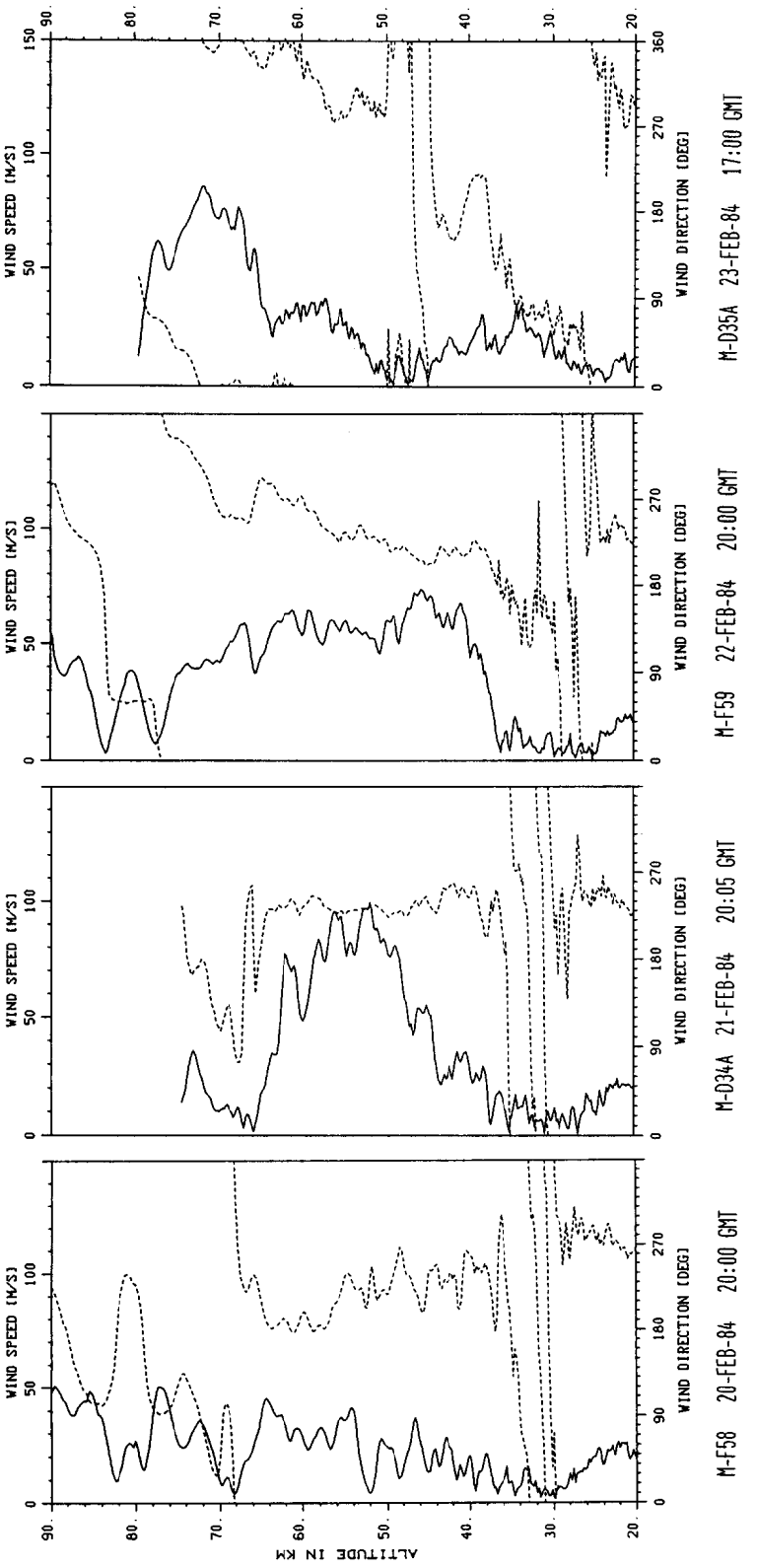

Fig. 3. Daily measurements of wind speed (solid) and direction (dotted) before and during the passage of the major stratospheric warming peak over Andøya on 23 Feb.

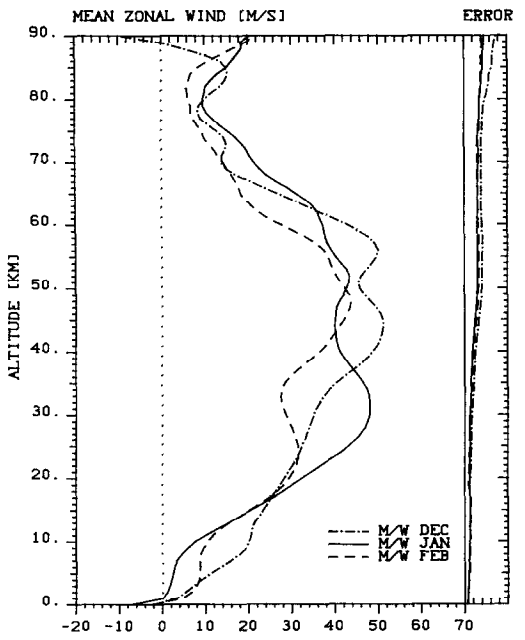

Fig. 4a. Monthly mean zonal winds of the MAP/WINE measurements over Andøya (M/W) and statistical error bar (right panel) on the same scale.

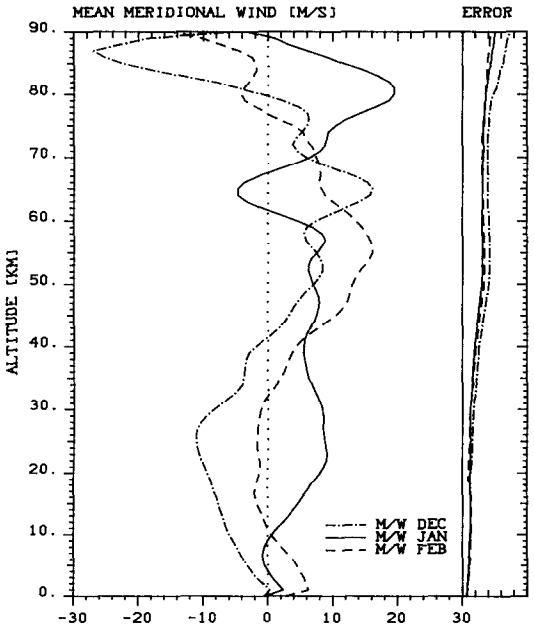

Fig. 4b. As Fig. 4a, but for the meridional component.

a linear decrease from 40 m s^{-1} at 60 km to 0 m s^{-1} at 80 km, which is almost identical to our January profile. A direct comparison with Poker Flat winds suffers, however, because there are quasi-stationary planetary waves which introduce systematic longitudinal differences in the zonal and meridional mean flow. These mainly orographically forced waves can propagate vertically up to mesospheric heights in winter (LABITZKE, 1980), whereas in summer they are trapped within the tropospheric westerlies. Thus, even long term averages of single station observations hardly reflect zonal averaged winds in winter.

An important step towards a better global data coverage probably comes from satellite data. A proposal for a revised COSPAR International Reference Atmosphere was given by BARNETT and CORNEY (1985). It is based on satellite measurements from June 1975 to July 1978 between 30 km and 80 km and from January 1973 to December 1974 between 15 km and 55 km, which were obtained using nadir scanning radiometers. In addition to extensive tables of temperatures, geopotential heights and geostrophic winds, average longitudinal variations were also resolved for the planetary wave numbers 1 and 2. We shall use the satellite derived winds for a comparison with our measurements. Although the geostrophic approximation lacks an Earth curvature correction at high latitudes, the uncorrected zonal geostrophic satellite winds are first compared with the observed mean winds for December, January and February in Fig. 5a. To compensate for the longitudinal deviation from the latitude mean at our location, the geostrophic zonal mean winds given by BARNETT and CORNEY (1985) were corrected for 16°E using their analysis of the geopotential height waves 1 and 2 between 60°N and 80°N. Good agreement is attained between the satellite and our measured zonal winds for the February mean. The January profiles deviate at some altitudes, but principally agree with regard to the magnitudes of the absolute stratopause maxima and the mesopause minimum. The December profiles strongly differ in the upper mesosphere by 30 m s^{-1} and more and in the stratopause region the satellite zonal geostrophic winds are still higher by 20 m s^{-1} than our December profile. We should note that the longitudinal correction acts generally to increase the satellite winds at Andøya by 3–10 m s^{-1} (strongest in December in the upper mesosphere with 10 m s^{-1}), except for the mesospause in January, when the correction is slightly negative.

Modifications to the geostrohic assumption for the satellite data are included in the following discussion. The wind components were computed from the equations of motion on a sphere (equations 2 and 3)

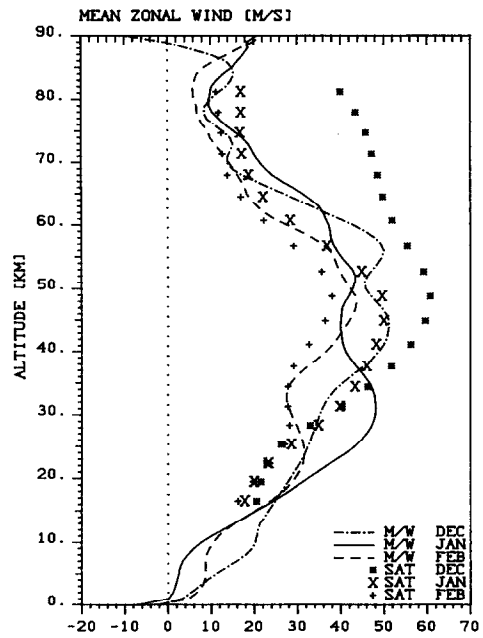

Fig. 5a. As Fig. 4a, but compared with geostrophic winds derived from satellite measurements (SAT) by BARNETT and CORNEY (1985) (proposal for a revised CIRA 1986) and corrected for 16°E.

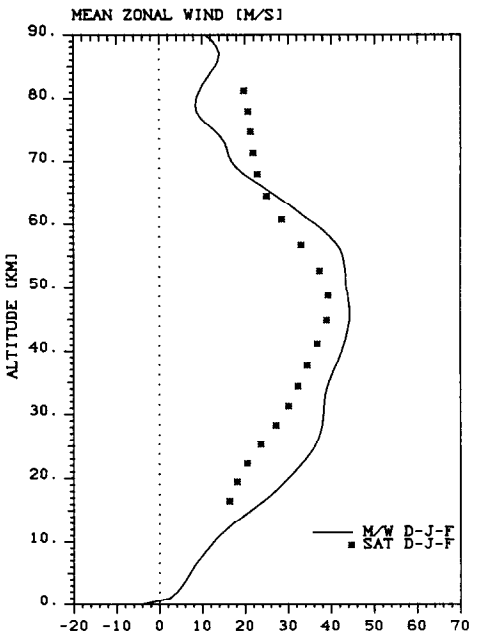

Fig. 5b. Winter mean zonal wind of the MAP/WINE measurements over Andøya (M/W) compared with winter average (Dec., Jan., Feb.) derived from satellite measurements (SAT) as in Fig. 5a, but applying equation 3.

assuming stationarity of the mean flow and of the superimposed waves of wave numbers 1 and 2. Only those terms which might lead to changes of more than $3\,\mathrm{m\,s^{-1}}$ were included. Yet unknown flux divergence terms may still cause a significant bias to the actual mean winds

$$v\cdot\left(f+\frac{u\cdot\tan\phi}{a}-\frac{1}{a}\frac{\partial u}{\partial\phi}\right)-fv_g-\frac{u}{a\cdot\cos\phi}\frac{\partial u}{\partial\lambda}=0, \tag{2}$$

$$\frac{u^2\tan\phi}{a}+f(u-u_g)=0. \tag{3}$$

The index g refers to geostrophic values which were obtained from satellite data as described above. f, a, ϕ and λ represent the Coriolis parameter, Earth radius, latitude and longitude, respectively. Our winter mean is compared with such a corrected satellite winter mean (December, January and February) in Fig. 5b. Above 60 km the difference between both data sets is caused by the large difference in December. Below 60 km the satellite winds are somewhat reduced compared to Fig. 5a, due to the spherical correction in equation 3. They are significantly lower than the MAP/WINE measurements by 4–$10\,\mathrm{m\,s^{-1}}$. This difference would have been reduced if the final development of the major warming at the end of February could have been included in our averaging period. The large deviation of $10\,\mathrm{m\,s^{-1}}$ in the lower stratosphere, however, is consistent with a strong winter circulation, at least at high latitudes, during the MAP/WINE winter (LABITZKE *et al.*, 1984).

A comparison of the monthly meridional wind components is shown in Fig. 6a. The satellite winds were computed from equation 2, which turns out to be almost identical to a purely geostrophic computation, since the correction terms effectively cancel each other. The meridional satellite winds simply reflect the amplitude of stationary waves and their average longitudinal position relative to our location. The good agreement in vertical shape of the December and February profiles with our mean profiles suggests that during these months of the MAP/WINE winter the location of the polar trough was close to its usual winter position. It also indicates stationary planetary waves to be the main cause for the long term meridional wind structure, at least up to 90 km. Nevertheless, we observed higher values in the mesosphere than the satellite winds indicate, which becomes evident comparing the winter averages in Fig. 6b. Our winter mean values exceed the satellite derived winds by 5–$10\,\mathrm{m\,s^{-1}}$ between 70 and 80 km.

In principle, the difference between the long term average of meridional wind measurements and satel-

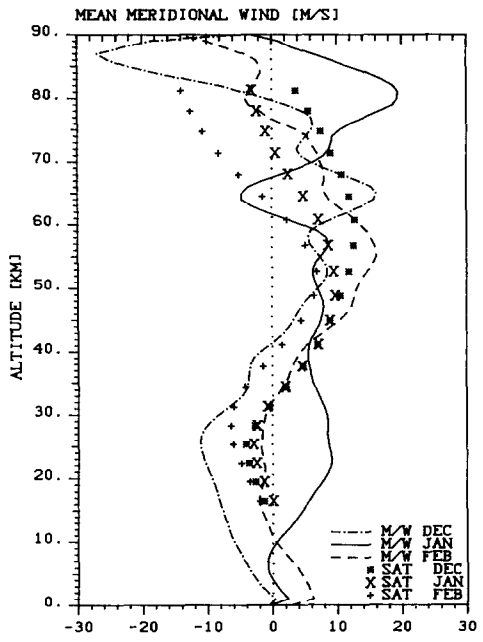

Fig. 6a. As Fig. 4b, but compared with meridional winds deduced from the wave number 1 and 2 analyses by BARNETT and CORNEY (1985) at 70°N, 16°E applying equation 2 (SAT).

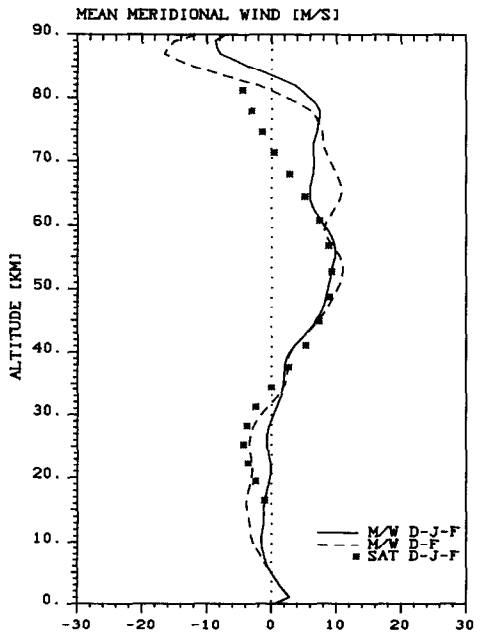

Fig. 6b. As Fig. 6a, but for the winter means (D–J–F) and the MAP/WINE winter mean for a selected period (D–F, see text).

lite winds at a single location should reflect ageostrophic motions. Due to the different years of observations and the limited averaging periods, it is, of course, uncertain that the difference in Fig. 6b actually reflects an ageostrophic flow. Obviously, one reason for this uncertainty is the irregular shape of the MAP/WINE January profile as compared with the satellite data. As reported by LABITZKE *et al.* (1984), wave 1 travelled westward between 11 Jan. and 10 Feb. 1984. This led to strong southerly winds over Andøya before 20 Jan. in the lower stratosphere, which is evident in Fig. 2 and which is the most striking dissimilarity if compared to the December and February winds. The center of the polar trough was located almost opposite to its usual position around 26 Jan. at 1 mb (PETZOLDT, 1985).

To reduce the contribution of this period—which is rather untypical of a long term average—to the winter mean, the data between 16 Jan. and 2 Feb. were excluded from averaging, as was the end of our observation period, namely the major warming peak. The results shown in Fig. 6b (denoted D–F) agree with the satellite winter mean below 60 km within our error bar. The northward flow relative to the satellite winds in the upper mesosphere is now shifted down to 60 km and the maximum values are slightly reduced to just below $10\,m\,s^{-1}$ at 77 km. Smoothing out some vertical fluctuations, probably due to unremoved long period variations (evident for example in the December winds at 65 km; Fig. 6a and Fig. 2), we obtain the following estimates of an ageostrophic poleward flow: $1\,m\,s^{-1}$ at 60 km, $4\,m\,s^{-1}$ at 65 km, $5\,m\,s^{-1}$ at 70 km, $8\,m\,s^{-1}$ at 75 km and $6\,m\,s^{-1}$ at 80 km. An error bar of $\pm 3\,m\,s^{-1}$ seems to be appropriate for these values, with regard to the uncertainty of our mean. An extrapolation to 85 km suggests $0 \pm 5\,m\,s^{-1}$ for that altitude. We should note that there are several other possibilities to make the data sets compatible with each other in the stratosphere and to infer an ageostrophic flow in the mesosphere. For example, taking the difference between the average of December and February of both data sets would lead to a flatter meridional wind cell than obtained above which is slightly shifted to lower altitudes, showing a maximum of $6\,m\,s^{-1}$ around 70 km. The above choice was to maximize the averaging period in order to limit the statistical error.

GROVES' (1969) estimate of a meridional winter circulation is generally similar to ours, but indicates only $5\,m\,s^{-1}$ maximum southerlies at 75 km at 70°N. The large negative values which he obtained below 60 km are probably due to an overemphasis on North American stations and are in an opposite direction to the positive meridional wind above Andøya.

5. DISCUSSION

One of the possible reasons for the differences between the winter mean winds over Andøya during 1983/1984 and the winter mean satellite winds over Andøya between 1973 and 1978 may be a long term variation of the winds due to a solar cycle dependence. SPRENGER and SCHMINDER (1969), using low frequency drift measurements around 95 km, observed the mean winds over central Europe to be stronger during solar maximum (10.7 cm flux of 200×10^{-22} W m^{-2} Hz^{-1}) than during solar minimum (70×10^{-22} W m^{-2} Hz^{-1}) by 20 m s^{-1} and 12 m s^{-1} for the zonal and meridional wind components, respectively. These results were later confirmed by PORTNYAGIN *et al.* (1977). However, the significance of this relationship appears to decrease if one includes the later 1980/1981 solar maximum (GREISIGER, 1983; DARTT *et al.*, 1983). The level of solar activity was moderate during the MAP/WINE winter, as indicated by a 10.7 cm flux of 91, 112 and 137×10^{-22} W m^{-2} Hz^{-1} in December, January and February, respectively, and slightly lower, 82, 85 and 97×10^{-22} W m^{-2} Hz^{-1}, for the respective months of the satellite measurements. Since the average relative flux difference is less than a quarter of the solar cycle variation based on the past 25 years, we regard solar cycle effects as of minor importance for our comparison. On the other hand, the interannual variability is usually larger than any secular variation within the altitude range 85–25 km, on which we focus particularly with regard to the zonal component.

We should mention, however, that Groves, in preparing the AFGL model atmosphere (GROVES, 1985), found some systematic latitudinal bias between the satellite measurements and previous models based on *in situ* temperature measurements. After Groves had corrected the satellite measurements by this difference (the relative change of this difference is less than 2 K for 10° latitude), the resulting geostrophic zonal winds were 10 m s^{-1} higher than the CIRA geostrophic winds at 70°N. Since we do not wish to give preference to either of the satellite model atmospheres (CIRA or AFGL), we are left with an uncertainty of about 5 m s^{-1} for the satellite derived zonal winds.

Our estimate of an ageostrophic meridional wind above northern Scandinavia is based on the assumption that the planetary wave structure can be extrapolated from the stratosphere to the mesosphere. This seems to be appropriate in our case, in view of the excellent agreement between our measurements and the satellite deduced meridional winds below 60 km. An unusual behaviour of planetary wave propagation into the mesosphere during the MAP/WINE winter cannot be excluded, but it seems unlikely to have lasted more than two months. Compared with the equatorward flow in summer, with maximum values of around 16 m s^{-1} at 88 km (NASTROM *et al.*, 1982), our estimates suggest a weaker meridional winter circulation over northern Scandinavia located 12 km below the summer wind cell.

LINDZEN (1981) suggested that breaking gravity waves are the main momentum source at high latitudes for this diabatic circulation. Forcing by planetary waves was found by HOLTON (1983) to have only secondary effects, on average. This author successfully modelled a realistic temperature and wind distribution using a parametrisation of gravity wave momentum deposition. The model yielded similar net meridional winds to those which we have estimated. Furthermore, MST radar measurements support the gravity wave breaking theory. The altitude region of echo occurrence coincides quite well with the region of meridional circulation in winter and summer (BALSLEY *et al.*, 1983; CZECHOWSKY and RÜSTER, 1985). Although the MST radar echo power cannot be regarded as a direct measure of turbulence intensity (THRANE *et al.*, 1987), it suggests the expected qualitative relationship between turbulence and breaking or dissipating (by turbulence) gravity waves.

6. SHORT TERM VARIABILITY

In view of the possible importance of gravity waves for the momentum budget of the middle atmosphere, we have briefly analysed the short term variability as indicated by rocket measurements during the MAP/WINE salvoes. According to equation 1 the average squared temporal differences of the wind components were computed for two different time lag intervals: 0–1.5 h and 1.5–5 h. Figures 7 and 8 show the results of two different samples. The first one (Fig. 7) includes 47 launches, two thirds of which were performed in the middle of February and one third in December and at the beginning of January. The rocket wind measurements during two salvoes on 13 Jan. and 21 Jan. comprise most of the data (36 launches) used in the second sample (Fig. 8). Figures 7a and 8a show the respective average over 5 km of the squared differences, which have been divided by 2 to obtain r.m.s. equivalent values, as usually quoted in the literature.

The short term variability of the wind is generally higher for sample 2 than for sample 1 above 45 km. The r.m.s amplitudes for time differences less than 1.5 h (average time lag is 0.8 h) are about 2–3 m s^{-1} at 30 km in both samples. They increase to values of 11 m s^{-1} at 60 km in sample 1 and 15 m s^{-1} at 65 km in

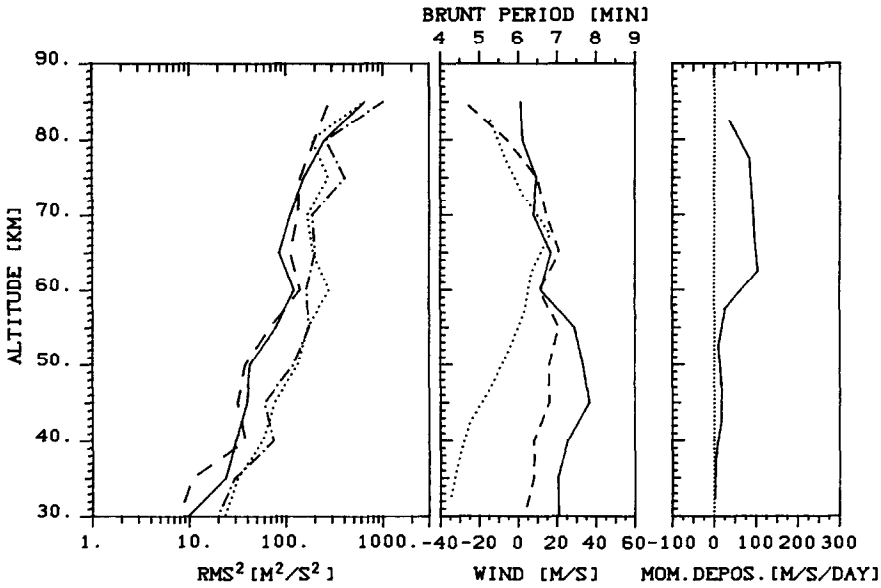

Fig. 7. Left panel (a): variances (r.m.s.^{2}) of the zonal (solid) and meridional (dashed) wind components for time lags < 1.5 h and between 1.5 h and 5 h (zonal component: dash-dotted, meridional component: dotted) using rocket measurements in December and February. Center (b): mean zonal (solid) and meridional (dashed) winds of the launches used in (a). The Brunt–Vaisala period (dotted) refers to an average temperature profile during the times of the launches used in (a). Right panel (c): momentum flux divergence calculated from equation 4 and using the results of (a).

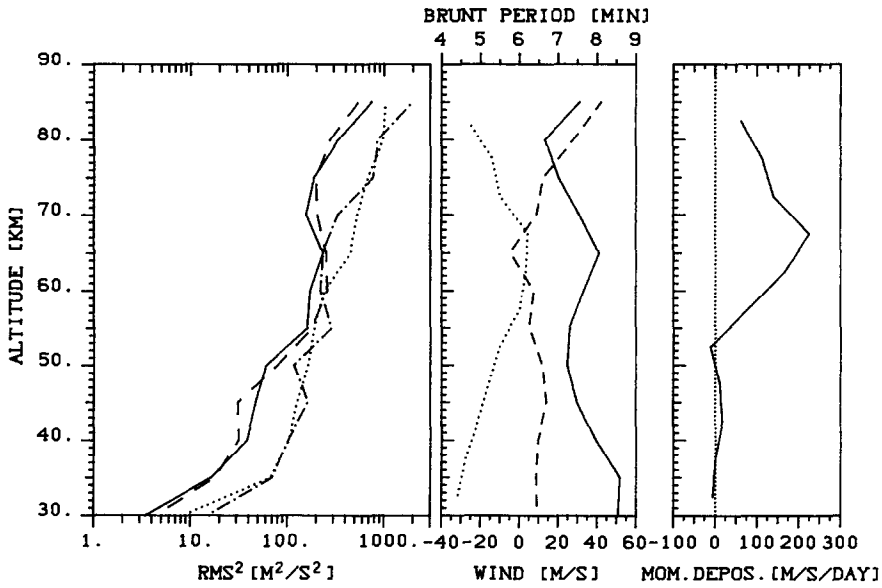

Fig. 8. As Fig. 7, but for launches during January.

sample 2. It is possible that the decrease of amplitudes above 65 km was partly caused by the limited vertical resolution of the spheres in the mesosphere, which, in contrast to the statistical error (see also Section 2), leads to an underestimate of the variances. However, both effects are of the same order of magnitude at 85 km.

The variances for time lag two (1.5–5 h, average time difference 2.7 h) should be at least of the order of the lag one results, because they should additionally

represent the variance contributions of long period waves. In Fig. 7 the variance contributions of long and short period waves seem to be of the same order of magnitude up to 75 km. From Fig. 8 dominating contributions of long period waves may be inferred in the upper mesosphere and around 45 km, as well as minimum contributions around 60 km.

A more quantitative separation of the squared differences for both time lags into contributions from two frequency ranges was obtained by assuming a shape of the power spectrum of the wind fluctuations vs. frequency. With a spectral index of -1.5 (CZECHOWSKY and RÜSTER, 1985), and taking into account the amplitude response of the applied difference filter at the time lags used, the frequency overlap of both time lags has been removed into contributions of the period ranges 0–3 h and 3–13 h. Under these assumptions the variance for lag one includes all contributions from the 0–3 h periods plus 20% of the long period variance, whereas the variance for time lag two represents all variance contributions from long periods > 3 h plus 70% of the short period range. Maximum response was found at periods around 1.6 h and at around 5.5 h for time lags one and two, respectively. These values are used in the following to obtain an order of magnitude estimate of the momentum deposition (MANSON *et al.*, 1975; VINCENT and STUBBS, 1977).

$$\frac{1}{\rho}\frac{\partial}{\partial z}(\rho\overline{u'w'}) \sim \frac{1}{\rho}\frac{\partial}{\partial z}\left(\rho\overline{u'^2}\frac{k}{m}\right) \sim \left(\frac{1}{H_u} - \frac{1}{H_D}\right)\overline{u'^2}\frac{\omega}{\omega_B}, \quad (4)$$

where ρ is the air density and $\overline{u'w'}$ is the temporal average of the product of the horizontal and vertical perturbation velocities. w' can be expressed as $u'k/m$ for vertical wavelengths which are much smaller than $2\pi H_D$, where H_D denotes the density scale height and k and m are the horizontal and vertical wave numbers, respectively. The dispersion relation for waves with periods much less than the inertial period but much longer than the Brunt–Vaisala period was used to substitute for k/m. H_u defines a scale height describing the exponential increase of the r.m.s. amplitude squared with altitude. The intrinsic frequency ω and the Brunt frequency ω_B were taken as constant with height. In order to reduce the scatter in the raw differences, both wind components, which show a very similar behaviour, were averaged and a 1-4-1 altitude smoothing was applied. The momentum deposition rates were then separately calculated for the above mentioned period ranges 0–3 h and 3–13 h according to equation 4 and added.

In employing equation 4 one assumes that one can represent the entire wave spectrum by a single upward propagating gravity wave. Since little is known so far about the distribution of horizontal phase velocities, we have to specify the fraction of the wave spectrum which transports negative momentum upwards. This fraction must exceed the upward transport of positive momentum to be able to decelerate the zonal flow, as required by the northward ageostrophic wind. If one assumes that 50% of the total variance causes the net deceleration of the mean flow (implying 25% to cause an acceleration) one obtains the net momentum deposition rates shown in Figs. 7c and 8c. The values vary from 50 to 200 $\mathrm{m\,s^{-1}\,day^{-1}}$ in the mesosphere and, on average, exceed the required forcing of 30–100 $\mathrm{m\,s^{-1}\,day^{-1}}$. It should be noted that observed frequencies were taken as intrinsic frequencies (required in equation 4). This may lead to an overestimate of, for example, the forcing in the stratosphere, where a weak 'wave breaking region' seems to be present around 45 km. Since inertio gravity waves are frequently observed here (HASS and MEYER, 1987), their advection by a strong background wind is likely to cause a bias of the intrinsic long periods to observed short periods. Also, reflection of waves at adiabatic lapse rates (HINES and REDDY, 1967; BRETHERTON, 1969), which may have been interpreted in this analysis as being absorbed, as well as horizontally ducted waves (CHIMONAS and HINES, 1986), may lead to an overestimate.

7. CONCLUSION

The wind measurements which were performed over northern Scandinavia during the MAP/WINE campaign are generally compatible with the mean winds derived from earlier satellite temperature measurements and proposed for the revised CIRA 1986. Although a single monthly mean value may not be typical of a long term average, our winter mean zonal winds reflect quite satisfactorily a slightly enhanced winter circulation at high latitudes. A comparison of the meridional wind measurements with satellite derived winds is proved to be necessary for a quantitative determination of an ageostrophic meridional flow in winter. The meridional ageostrophic flow, which we have estimated, is consistent with the observed short time variability if one anticipates roughly 70% of the total variance to be due to saturating gravity waves which transport negative momentum upwards.

Acknowledgement—We gratefully acknowledge the continuous support of this research by Prof. U. VON ZAHN. We would also like to thank Dr K. H. FRICKE for reading the manuscript and Dr K. PETZOLDT for helpful suggestions. This investigation was supported by the Deutsche Forschungsgemeinschaft, Bonn–Bad Godesberg through grant Za 83 and the Bundesministerium für Forschung and Technologie, Bonn, through grant WRK 275. One of us, JR, acknowledges the very efficient cooperation with all EISCAT staff members, particularly during MAP/WINE. The EISCAT Scientific Association is supported by the Centre National de la Recherche Scientifique, France, Suomen Akatemia, Finland, Max-Planck Gesellschaft, F.R.G., Norges Almenvitenskapelige Forskningsrad, Norway, Naturvetenskapliga Forskningsradet, Sweden, and Science and Engineering Research Council, U.K.

REFERENCES

BALSLEY B. B., ECKLUND W. L. and FRITTS D. C. 1983 *J. atmos. Sci.* **40,** 2451.

BARNETT J. J. and CORNEY M. 1985 *Handbook for MAP* **16,** 47.

BRETHERTON F. P. 1969 *Q. J. R. met. Soc.* **95,** 213.

CHIMONAS G. and HINES C. O. 1986 *J. geophys. Res.* **91,** 1219.

CIRA 1972 *COSPAR International Reference Atmosphere* 1972, p. 139. Akademie-Verlag, Berlin.

CZECHOWSKY P. and RÜSTER R. 1985 *Handbook for MAP* **18,** 207.

CZECHOWSKY P., RÜSTER R. and SCHMIDT G. 1984 *Adv. Space Res.* **4** (4), 47.

DARTT D., NASTROM G. and BELMONT A. 1983 *J. atmos. terr. Phys.* **45,** 707.

GREISIGER K. M. 1983 Ground based studies of the middle atmosphere at the observatory of ionospheric research in Kühlungsborn, p. 35. HHI-STP-Report no. 17, Berlin.

GROVES G. V. 1969 *J. Br. interplanet. Soc.* **22,** 285.

GROVES G. V. 1985 Technical Report, Air Force Geophysics Laboratory, Hanscom AFB, MA 01731, AFGL-TR-85-0129.

HASS H. and MEYER W. 1987 *J. atmos. terr. Phys.* **49,** 705.

HINES C. O. and REDDY C. A. 1967 *J. geophys. Res.* **72,** 1015.

HOLTON J. R. 1983 *J. atmos. Sci.* **40,** 2497.

LABITZKE K. 1980 *Phil. Trans. R. Soc.* **A296,** 7.

LABITZKE K., NAUJOKAT B., PETZOLDT K., LENSCHOW R. and O'NEILL A. 1984 *Beil. Berl. Wettkarte* **S015/84,** 1.

LABITZKE K., MANSON A. H., MULLER H. G., RAPOPORT Z. and WILLIAMS E. R. 1987 *J. atmos. terr. Phys.* **49,** 639.

LINDZEN R. S. 1981 *J. geophys. Res.* **86,** 9707.

MANSON A. H., GREGORY J. B. and STEPHENSON D. G. 1975 *J. atmos. Sci.* **32,** 1682.

MANSON A. H., MEEK C. E., MASSEBEUF M., FELLOUS J. L., ELFORD W. G., VINCENT R. A., CRAIG R. L., ROPER R. G., AVERY S., BALSLEY B. B., FRASER G. J., SMITH M. J., CLARK R. R., KATO S., TSUDA T. and EBEL A. 1985 *Adv. Space Res.* **5** (7), 135.

MASSEBEUF M., BERNARD R., FELLOUS J. L. and GLASS M. 1979 *J. atmos. terr. Phys.* **41,** 647.

MEYER W. 1985 *Seventh ESA Symposium on European Rocket and Balloon Programmes and Related Research*, p. 55. ESA SP-229.

MEYER W., GERNDT R., PHILBRICK C. R. and SCHMIDLIN F. J. 1985 *Seventh ESA Symposium on European Rocket and Balloon Programmes and Related Research*, p. 41. ESA SP-229.

MULLER H. G., WHITEHURST G. A. and O'NEILL A. 1985 *J. atmos. terr. Phys.* **47,** 1143.

NASTROM G. D., BALSLEY B. B., CARTER D. A. 1982 *Geophys. Res. Lett.* **9,** 139.

OFFERMANN D. 1985 *J. atmos. terr. Phys.* **47,** 1.

OFFERMANN D., GERNDT R., KÜCHLER R., BAKER K., PENDLETON W. R., MEYER W., VON ZAHN U., PHILBRICK C. R. and SCHMIDLIN F. J. 1987 *J. atmos. terr. Phys.* **49,** 655.

PETZOLDT K. 1985 *Seventh ESA Symposium on European Rocket and Balloon Programmes and Related Research*, p. 33. ESA SP-229.

PORTNYAGIN YU. I., KAIDALOV O. V., GREISIGER K. M. and SPRENGER K. 1977 *Phys. Solariterr. Potsdam* **1977** (5), 91.

RÖTTGER J. and MEYER W. 1987 *J. atmos. terr. Phys.* **49,** 689.

RÜSTER R. 1984 *Adv. Space Res.* **4** (4), 3.

RÜSTER R. and KLOSTERMEYER J. 1987 *J. atmos. terr. Phys.* **49,** 743.

SCHMIDLIN F. J. and MICHEL W. R.	1985	*Seventh ESA Symposium on European Rocket and Balloon Programmes and Related Research*, p. 49. ESA SP-229.
SCHMIDLIN F. J., CARLSON M., REES D., OFFERMANN D., PHILBRICK C. R. and WIDDEL H.-U.	1985	*J. atmos. terr. Phys.* **47,** 183.
SPRENGER K. and SCHMINDER R.	1969	*J. atmos. terr. Phys.* **31,** 217.
THRANE E. V., BLIX T. A., HALL C., HANSEN T. L., VON ZAHN U., MEYER W., CZECHOWSKY P., SCHMIDT G., WIDDEL H.-U. and NEUMANN A.	1987	*J. atmos. terr. Phys.* **49,** 751.
VINCENT R. A. and STUBBS T. J.	1977	*Planet. Space Sci.* **25,** 441.
WIDDEL H.-U.	1987	*J. atmos. terr. Phys.* **49,** 723.
VON ZAHN U.	1987	*J. atmos. terr. Phys.* **49,** 607.